

Inelastic Reactions in Proton-Deuteron Scattering at 1.825 and 2.11 GeV/c

D. C. BRUNT,* M. J. CLAYTON,† AND B. A. WESTWOOD

Cavendish Laboratory, Cambridge, England

(Received 4 March 1969)

The final states $p_s p p \pi^-$, $p_s p p \pi^- \pi^0$, $p_s p n \pi^+ \pi^-$, and $n_s p p \pi^+ \pi^-$ have been observed in pd collisions at 1.825 and 2.11 GeV/c. The spectator-nucleon momentum and angular distributions are shown to require the addition of double-scattering events to the usual impulse-model predictions, in proportions varying between 15 and 40%. Results for the reaction $pn \rightarrow p p \pi^-$ are in good agreement with the one-pion-exchange model. The cross section for the $T=0$ part of the reaction $pn \rightarrow p n \pi^+ \pi^-$ rises by 0.92 ± 0.22 mb between 1.825 and 2.11 GeV/c, compared with a rise of 3 mb in the total $T=0$ nucleon-nucleon cross section in the same energy region; but no evidence has been found for the reaction $pn \rightarrow NN^*(1470)$.

I. INTRODUCTION

LITTLE previous work has been reported on proton-neutron interactions above a kinetic energy of 970 MeV.¹ Accurate total-cross-section measurements exist in the momentum range 1.1–8 GeV/c,² but apart from bubble-chamber experiments at 3.7³ and 7 GeV/c,⁴ there has been no detailed study of inelastic processes.

This paper presents data on the p - n interaction as studied in pd collisions at incident proton momenta of 1.825 and 2.110 GeV/c, chosen in order to examine the onset of the rise in the $T=0$ nucleon-nucleon total cross section between 1.5 and 3 GeV/c,² and to detect any association of this rise with $N^*(1470)$ production.

II. EXPERIMENTAL PROCEDURE

The experiment was carried out at the NIMROD proton synchrotron, using the 80-cm Saclay bubble chamber filled with deuterium. Double pulsing was used to get two pictures from each machine pulse and approximately 28 000 useful pictures were obtained at each incident momentum.

Since the interesting reactions for the study of the p - n interaction:

$$p+d \rightarrow p_s+p+p+\pi^- \quad (1)$$

$$\rightarrow p_s+p+p+\pi^-+\pi^0 \quad (2)$$

$$\rightarrow p_s+p+n+\pi^++\pi^-, \quad (3)$$

all involve a spectator proton p_s , the initial scanning procedure was aimed at preferentially selecting events containing them. The following types of event were measured at first:

(i) All three-prong events with no obvious π^+ track. Three-prong events have a spectator proton with a track too short to be visible. The presence of a π^+ shows that the event cannot be of type (1), the only type which can be kinematically fitted under these circumstances.

(ii) Four-prong events with one proton of momentum < 400 MeV/c (as determined by template and bubble-density measurements on the scanning table). At a later stage the rejected four-prong events were also measured in order to investigate the spectator-nucleon problem by comparing the reaction

$$p+d \rightarrow n_s+p+p+\pi^++\pi^- \quad (4)$$

(involving a spectator neutron n_s) with previous experiments⁵ on scattering from free protons at similar energies.

The following reactions involving deuterons in the final state were also studied:

$$p+d \rightarrow p+d+\pi^++\pi^- \quad (5)$$

$$\rightarrow p+d+\pi^++\pi^-+\pi^0 \quad (6)$$

$$\rightarrow n+d+\pi^++\pi^++\pi^-. \quad (7)$$

Even with all the four-prong events measured, there was still some bias against events with a deuteron and a slow proton, but this was well understood and allowed for appropriately. Results for the final states containing deuterons, including evidence for a d - π^+ resonance, have already been published.⁶

The over-all scanning efficiency was determined, by rescanning a portion of the film, to be 92.6% independent of the topology.⁷

The events were measured on two conventional semi-automatic film-plane digitized and processed by the

* Present address: Patent Office, London, England.

† Present address: TC Division, CERN, Geneva, Switzerland.

¹ J. G. Rushbrooke, D. V. Bugg, A. J. Oxley, J. A. Zoll, M. Jobs, J. Kinson, L. Riddiford, and B. Tallini, *Nuovo Cimento* **33**, 1509 (1964). This paper contains references to earlier work at lower energies.

² D. V. Bugg, D. C. Salter, G. H. Stafford, R. F. George, K. F. Riley, and R. J. Tapper, *Phys. Rev.* **146**, 980 (1966).

³ (a) W. M. Bugg, G. T. Condo, H. O. Cohn, and R. D. McCulloch, *Bull. Am. Phys. Soc.* **12**, 470 (1967); (b) H. O. Cohn, R. D. McCulloch, W. M. Bugg, and G. T. Condo, *Phys. Letters* **26B**, 598 (1968).

⁴ A. Shapira, O. Benary, Y. Eisenberg, E. E. Ronat, D. Yaffe, and G. Yekutieli, *Phys. Rev. Letters* **21**, 1835 (1968).

⁵ (a) E. Pickup, D. K. Robinson, and E. O. Salant, *Phys. Rev.* **125**, 2091 (1962); (b) E. L. Hart, R. I. Louttit, D. Luers, T. W. Morris, W. J. Willis, and S. S. Yamamoto, *ibid.* **126**, 747 (1962); (c) D. V. Bugg, A. J. Oxley, J. A. Zoll, J. G. Rushbrooke, V. E. Barnes, J. B. Kinson, W. P. Dodd, G. A. Doran, and L. Riddiford, *ibid.* **133**, B1017 (1964); (d) A. M. Eisner, E. L. Hart, R. I. Louttit, and T. W. Morris, *ibid.* **138**, B670 (1965).

⁶ D. C. Brunt, M. J. Clayton, and B. A. Westwood, *Phys. Letters* **26B**, 317 (1968).

⁷ D. C. Brunt, Ph.D. thesis, University of Cambridge, 1967 (unpublished).

CRAB series of analysis programs.⁸ The beam momentum was determined both by direct measurement of beam tracks and by kinematic fitting of type-(1) events, treating the beam momentum as an unknown. The use of bubble-density estimates enabled most events to be uniquely identified with one of the final states (1)-(7), and after remeasurements no more than 2% of events still had ambiguous identifications.

The numbers of events in each final state are summarized in Table I and include a small number of events which, although identified with a particular final state, failed the kinematic fitting and are therefore not included in the histograms.

III. DEUTERON AS NEUTRON TARGET

The use of the deuteron as a neutron target is based on the validity of the impulse approximation,⁹ which states that, because of the large radius and small binding energy of the deuteron, an incident particle effectively interacts with only one of the nucleons at a time. The effect of the deuteron binding on cross-section measurements has been considered by Glauber and others.¹⁰

A. Spectator Distributions

In the simplest form of the impulse approximation, the spectator nucleon is unaffected by the interaction taking place on the other nucleon in the deuteron, and it follows that, in the laboratory system, the spectator's angular distribution should be isotropic and its momentum distribution simply the Fourier transform of the spatial deuteron wave function.

Spectator nucleons are observed in final states (1)-(4), but there are few events of type (2), and only events of type (3) with visible spectator-proton tracks (i.e., momentum $\gtrsim 80$ MeV/c) can be fitted. Final states (3) and (4) are of course identical, except for the identification of different nucleons as the spectator. In all cases, the nucleon with least laboratory momentum

TABLE I. Number of events in each final state.

Final state	Number of events	
	1.825 GeV/c	2.110 GeV/c
$p_s p p \pi^-$	1379	1362
$p_s p p \pi^- \pi^0$	48	97
$p_s p n \pi^+ \pi^-$ ^a	300	564
$n_s p p \pi^+ \pi^-$ ^a	233	495
$p d \pi^+ \pi^-$	136	129
$p d \pi^+ \pi^- \pi^0$ and $n d \pi^+ \pi^- \pi^0$	2	14

^a Spectator identified as nucleon with smallest lab momentum (see text).

⁸ B. A. Westwood, Cambridge University Bubble Chamber Group Internal Reports, 1964-1967 (unpublished).

⁹ G. F. Chew, Phys. Rev. **80**, 196 (1950); **84**, 710 (1951); G. F. Chew and G. C. Wick, *ibid.* **85**, 636 (1952).

¹⁰ (a) V. Franco and R. J. Glauber, Phys. Rev. **142**, 1195 (1966); (b) R. J. Glauber, *ibid.* **100**, 242 (1955); D. R. Harrington, *ibid.* **135**, B358 (1964); **137**, AB3(E) (1965).

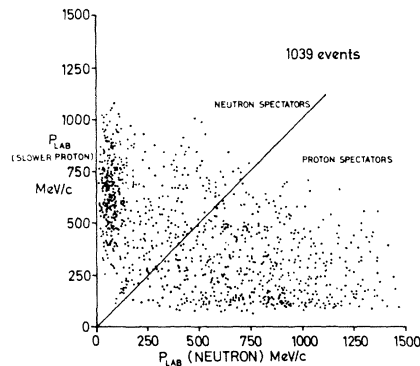


FIG. 1. Scatter plot of laboratory momenta in the final state $np\bar{p}\pi^+\pi^-$ at 2.11 GeV/c: slower of the two protons versus neutron. The identification of the spectator nucleon is shown by the diagonal line.

was identified as the spectator. This is the least biased method of assignment, and any other method of identification must shift the spectator laboratory-momentum distribution toward higher values.¹¹

A scatter plot is shown in Fig. 1 to illustrate the separation of final states (3) and (4), where either the neutron or the slower of the two protons may be the spectator. The cluster of events with spectator neutrons is obvious, but the corresponding cluster with spectator protons does not stand out so clearly, because the low-momentum spectators are missing. It is also clear that for some events neither nucleon is an obvious spectator.

Spectator-laboratory-momentum plots for events of types (1) and (4) are shown in Fig. 2. Curves corresponding to the Hulthén¹² and repulsive-core¹³ deuteron wave functions are shown in the inset of Fig. 2(a), normalized to the proportion of impulse-approximation events found by the least-squares fitting discussed below. The main plots show the phase-space distribution for the slowest nucleon from the final state $p\bar{p}p\pi^-$ or $n\bar{p}p\pi^+\pi^-$, where no assumption has been made that one of the nucleons is a spectator, which is intended to approximate the distribution for double-scattering events, in which the incident proton interacts with both nucleons in the deuteron. This curve is normalized to all events.

At low momenta, the repulsive-core wave function seems to give the better fit to the data, but neither wave function can account for the tail above 300 MeV/c. This tail has a similar shape to the phase-space distribution and it seems reasonable to identify events in the tail as ones in which double scattering has taken place. A knowledge of the proportion of double scattering is important for cross-section calculations, and so a

¹¹ A statistical-model calculation, assuming the impulse approximation, for the $np\bar{p}\pi^+\pi^-$ final state at 2.11 GeV/c gives the possibility of misidentification as less than 0.6% for spectator nucleons with momentum >150 MeV/c. The misidentification of slower spectators is even less likely.

¹² L. Hulthén and M. Sugawara, in *Handbuch der Physik*, edited by S. Flügge (Springer-Verlag, Berlin, 1957), Vol. 39, p. 1.

¹³ L. Durand, Phys. Rev. **123**, 1393 (1961).

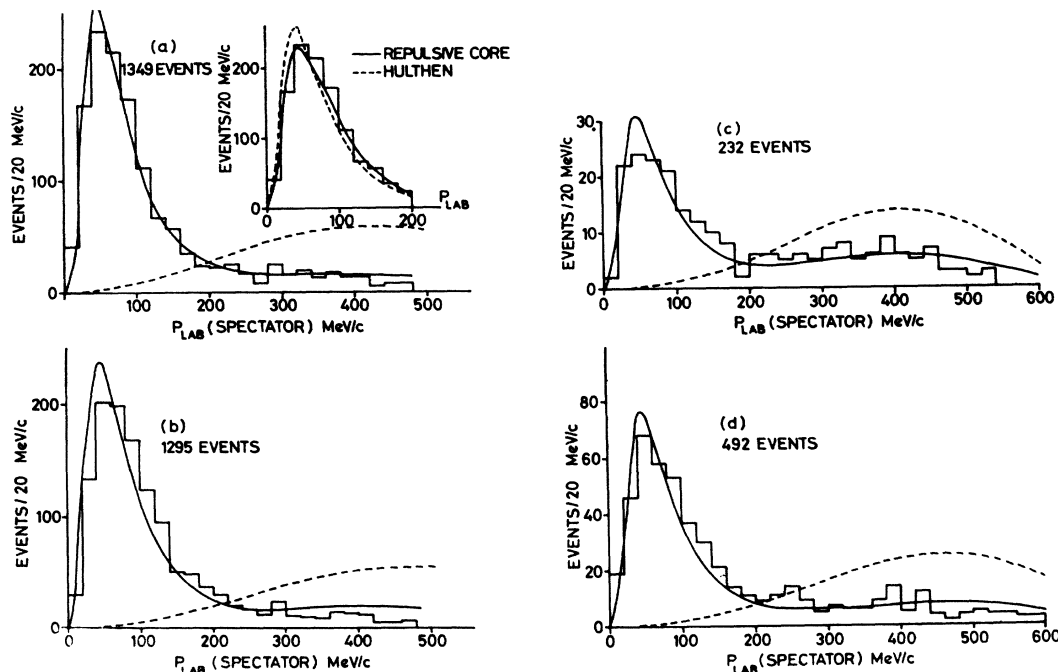


FIG. 2. Spectator-nucleon laboratory-momentum distributions: (a) $p_s p p \pi^-$ at 1.825 GeV/c; (b) $p_s p p \pi^-$ at 2.11 GeV/c; (c) $n_s p p \pi^+ \pi^-$ at 1.825 GeV/c; (d) $n_s p p \pi^+ \pi^-$ at 2.11 GeV/c. The dashed lines are phase-space distributions for $p p p \pi^-$ or $n p p \pi^+ \pi^-$, normalized to all events. The solid lines are the results of least-squares fits described in the text. The inset to (a) shows the Hulthén (dotted) and repulsive-core (solid) momentum distributions, normalized to the number of impulse-approximation events.

least-squares fit was made to the spectator momentum distribution, using various proportions of the Hulthén and phase-space predictions. (Replacing the Hulthén distribution by that for the repulsive-core wave function made no significant difference, since these two distributions only differ appreciably at low momenta, where the phase-space distribution is very small.) The results, as shown in Table II, together with the corresponding curves in Fig. 2, reveal a higher proportion of double scattering for final state (4) (double-pion

production) than for final state (1) (single-pion production), but little variation with energy.

Figure 3 shows scatter plots of spectator laboratory angle (calculated with respect to the beam direction) against laboratory momentum, for final states (1), (3), and (4) at 2.11 GeV/c. Clearly only the very-lowest-momentum spectators have a distribution which is at all isotropic, and as the spectator momentum increases there is more and more peaking in the forward direction. The distributions at 1.825 GeV/c are very similar,

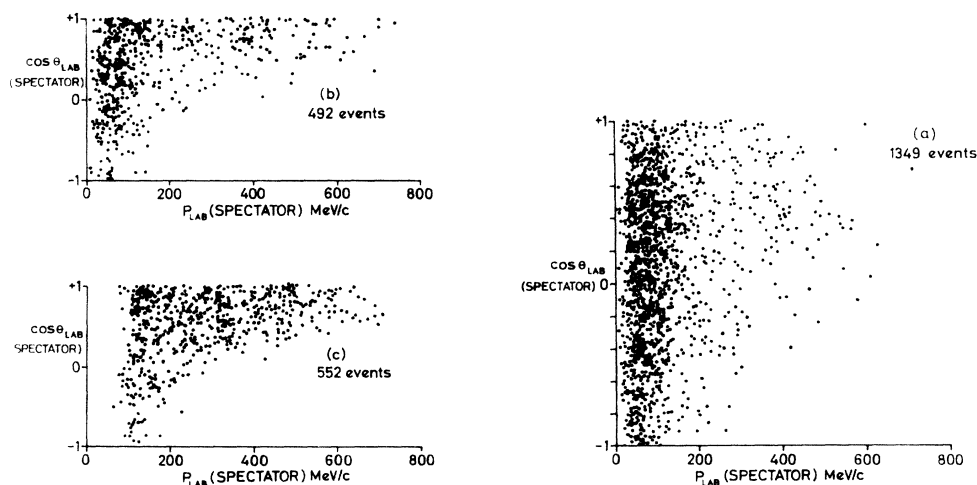


FIG. 3. Scatter plots for spectator nucleons at 2.11 GeV/c: laboratory angle versus laboratory momentum. (a) $p_s p p \pi^-$; (b) $n_s p p \pi^+ \pi^-$; (c) $p_s n p \pi^+ \pi^-$.

TABLE II. Amount of double scattering as deduced from the spectator momentum distribution, together with predicted and observed asymmetries for the spectator-nucleon angular distribution.

Final state	Incident momentum (GeV/c)	Percentage of double scattering	χ^2 value of the fit	Degrees of freedom	Predicted asymmetry	Observed asymmetry
$p_s p p \pi^-$	1.825	15±3	22.9	23	0.202	0.29±0.04
	2.110	17±5	50.0	23	0.201	0.24±0.04
$n_s p p \pi^+ \pi^-$	1.825	41±8	13.5	30	0.488	0.75±0.08
	2.110	31±7	27.1	37	0.393	0.57±0.05

and the same effect has also been observed in a $\bar{p}d$ experiment at 1.67 GeV/c.¹⁴ Table III summarizes the data in terms of an asymmetry parameter ϵ defined as $(F-B)/(F+B)$, where F and B are the numbers of events with spectators in the forward and backward hemispheres.

The theoretical predictions are from Monte Carlo calculations, carried out by generating random events according to several different models of the interaction.¹⁵ (A modified version of the program FOWL¹⁶ was used.) Calculations were made using three versions of the statistical model, with the following different assumptions about the spectator nucleon:

- (i) Its momentum and angular distributions are both as deduced from the Hulthén deuteron wave function.
- (ii) Its angular distribution is isotropic, but its momentum has the experimental distribution of Fig. 2.
- (iii) There is no spectator nucleon as such, and the available energy is simply shared in the usual way among all the final-state particles. (As stated above, this model should approximately reproduce the effects of double scattering.) Results from one-pion-exchange model (OPEM) calculations, which are discussed below in more detail, are also included in Table III. [Assumption (i) about the spectator nucleon was used in these calculations.] Complete angular-distribution predic-

tions from the various models are compared with experiment in Fig. 4.

Although the models involving spectators produce some forward peaking, this is insufficient to agree with the data. Assumption (ii) produces slightly more peaking than assumption (i), because the experimental distribution has an excess of high-momentum spectators, but it still falls short of that observed experimentally. This supports the view that the high-momentum tail is due to double scattering, and not to lack of knowledge of the exact form of the deuteron wave function at small distances (large Fermi momenta).

Double-pion-production reactions show a larger spectator angular-distribution asymmetry than single-pion production. Much of this is accounted for by the fact that the double-pion-production cross sections are still rising rapidly at these energies (which are only 200–300 MeV above threshold), whereas the cross section for single-pion production has leveled off. (The cross sections are shown below in Fig. 9.) Events in which the spectator proton (neutron) is traveling in the same direction as the incident proton will have a higher pn (pp) center-of-mass energy, so that a rising cross section will produce an effect in the required direction. It will be particularly marked for the $p_s n p \pi^+ \pi^-$ final state, where all the low-momentum spectators are

TABLE III. Observed and predicted spectator-nucleon angular-distribution asymmetries for various spectator-momentum cuts.

Final state	Incident momentum (GeV/c)	Spectator-momentum cut (MeV/c)	Observed asymmetry	Predicted values of asymmetry			OPEM
				Statistical model			
				Assumption (i)	Assumption (ii)	Assumption (iii)	
$p_s p p \pi^-$	1.825	<150	0.19±0.04	0.080	0.083	...	0.030
		>150	0.64±0.08	0.283	0.423	0.842	0.049
	2.110	None	0.29±0.04	0.093	0.142	0.823	0.031
		<150	0.17±0.04	0.063	0.056	...	-0.001
		>150	0.48±0.04	0.271	0.420	0.829	0.008
		None	0.24±0.04	0.076	0.134	0.814	-0.0005
$n_s p p \pi^+ \pi^-$	1.825	None	0.75±0.08	0.152	...	0.974	...
	2.110	<150	0.37±0.06	0.138	0.123	...	0.178
		>150	0.92±0.10	0.515	0.634	0.971	0.654
		None	0.57±0.05	0.162	0.255	0.910	0.207
$p_s p n \pi^+ \pi^-$	1.825	None	0.93±0.08	0.369	...	0.974	...
		<200	0.39±0.07	0.237
	2.110	>200	0.96±0.08	0.599	...	0.981	...
		None	0.74±0.05	0.269	...	0.964	...

¹⁴ D. M. Sendall, Ph.D. thesis, University of Cambridge, 1966 (unpublished).

¹⁵ M. J. Clayton, Ph.D. thesis, University of Cambridge, 1968 (unpublished).

¹⁶ F. James, CERN Report No. Th.68-15, 1968 (unpublished). A FORTRAN listing obtained from Imperial College, London, was used and modified.

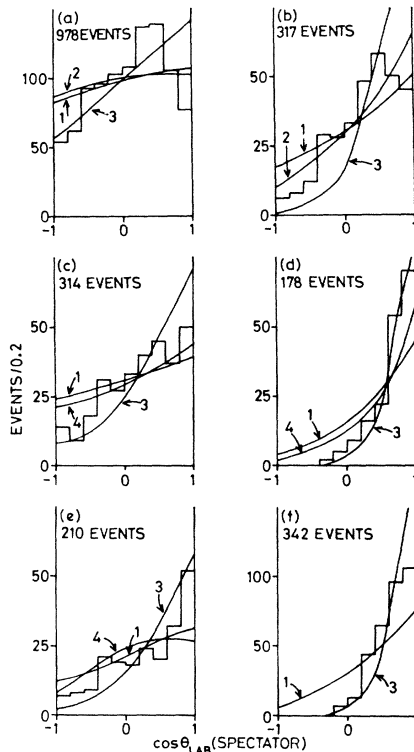


FIG. 4. Spectator-nucleon angular distributions at 2.11 GeV/c: (a) $p_s p p \pi^-$, spectator momentum <150 MeV/c; (b) $p_s p p \pi^-$, spectator momentum >150 MeV/c; (c) $n_s p p \pi^+ \pi^-$, spectator momentum <150 MeV/c; (d) $n_s p p \pi^+ \pi^-$, spectator momentum >150 MeV/c; (e) $p_s n p \pi^+ \pi^-$, spectator momentum <200 MeV/c; (f) $p_s n p \pi^+ \pi^-$, spectator momentum >200 MeV/c. The curves correspond to the following calculations, discussed in the text: (1) statistical model, assumptions (i); (2) statistical model, assumptions (ii); (3) statistical model, assumption (iii); (4) OPEM.

missing. The double-pion-production cross sections are not well known as a function of energy in this region, but since their rise is largely a reflection of the increase in available phase space, the statistical-model calculations may be used to give a rough guide to the size of the effect. The results for the final states $n_s p p \pi^+ \pi^-$ and $p_s p p \pi^-$ at 2.11 GeV/c, with a spectator-momentum cut of <150 MeV/c applied in each case to avoid effects due to different amounts of double scattering, both show an experimental asymmetry which is larger than the statistical-model [assumption (i)] prediction. On subtracting the latter, we are left with residual asymmetries of 0.24 ± 0.08 and 0.11 ± 0.05 , respectively. These figures show that while we have a trend in the right direction, a much more detailed knowledge of the cross sections is necessary before one can determine whether their variation with energy satisfactorily accounts for the whole of the difference between the single- and double-pion spectator angular-distribution asymmetries.

In the last two columns of Table II the over-all spectator angular-distribution asymmetry, with no spec-

tator momentum cut, is compared with the predicted value if the events are assumed to consist of impulse-approximation and double-scattering contributions in the proportions found in the least-squares fitting. Again the prediction shows the right trend but is too small, in this case sometimes by several standard deviations. A recent paper by Schwarzschild,¹⁷ concerned with the effect of the flux factor on impulse-model calculations, suggests that it is possible to have a spectator angular-distribution asymmetry of some 7% even if the cross section does not vary with energy. This may account for at least some of the discrepancy.

B. Final-State Interactions

The invariant masses of the spectator neutron and the slower of the two protons (in the laboratory), in events of the type $n_s p p \pi^+ \pi^-$, are found to peak at low values, especially for those events with high-momentum spectators. A final-state interaction between the two nucleons, which would be largest for small relative momenta,¹⁸ is a possible explanation. The OPEM and statistical-model [assumption (i)] calculations of Sec. III A were therefore modified to include such an interaction and the effects on the spectator angle and momentum distributions investigated.

Following Delbourgo,¹⁹ and assuming the dominance of one partial wave, the matrix element was written as

$$M = M_0 \left(1 + C \frac{e^{i\delta} \sin \delta}{2q/\omega} \right),$$

where M_0 is the matrix element without final-state interaction, δ the phase shift, q the relative momentum of the two nucleons in their center-of-mass system, and ω their invariant mass. The 1S_0 and 3S_1 partial waves were assumed to be dominant for the $T=0$ and $T=1$ parts of the interaction, respectively, and their values were taken from recent analyses of the nucleon-nucleon interaction.²⁰ The constant C , which expresses the strength of the interaction, is usually assumed to be roughly equal to one nucleon mass, but in this calculation values between 0.04 and 0.2 GeV/c² were found necessary in order to obtain agreement with experiment.

Typical results are shown in Fig. 5. An effect in the right direction is produced, though it is not possible to fit both the invariant-mass and the spectator-angle distributions in detail with the same parameters. The effect on the spectator-momentum distribution is to produce a slight high-momentum tail, much smaller than that observed experimentally.

¹⁷ B. M. Schwarzschild (unpublished report).

¹⁸ R. J. N. Phillips, Nucl. Phys. **53**, 650 (1964).

¹⁹ R. Delbourgo, Nucl. Phys. **38**, 281 (1962).

²⁰ M. H. MacGregor and R. A. Arndt, Phys. Rev. **139**, B362 (1965); H. P. Noyes, D. S. Bailey, R. A. Arndt, and M. H. MacGregor, *ibid.* **139**, B380 (1965).

The addition of an $n_s\pi^-$ final-state interaction had very little effect on the spectator distributions. This is probably due to the absence of large phase shifts in the $\pi-N$ system at very small relative momenta.

C. Comparison of $pd \rightarrow n_s p p \pi^+ \pi^-$ and $pp \rightarrow p p \pi^+ \pi^-$

The most suitable of the hydrogen-bubble-chamber studies of $pp \rightarrow p p \pi^+ \pi^-$ for comparison with the $n_s p p \pi^+ \pi^-$ events of this experiment is that of Pickup, Robinson, and Salant^{5(a)} at 2-GeV kinetic energy. (This experiment is referred to hereafter as PRS.) The corresponding pp center-of-mass energy is 2.697 GeV, compared with central values of 2.369 and 2.469 GeV in the present experiment.²¹ The main observations in PRS are (i) forward-backward peaking in the proton center-of-mass angular distribution, characteristic of a peripheral interaction, and (ii) resonance formation, with the $\Delta(1236)$ strong in the $p\pi^+$ system, but less marked in the $p\pi^-$. There is also some evidence for the existence of $N^*(1512)$ and $N^*(1688)$ in the $p\pi^-$ system.

Ferrari²² has successfully compared the PRS results (and also those of Hart *et al.*^{5(b)}) at a pp center-of-mass energy of 2.978 GeV with OPEM calculations. These calculations were repeated for the present experiment, allowing for the effect of the spectator neutron in varying the pp center-of-mass energy. The calculated total cross section was found to depend very sensitively on the exact form of this variation, and was difficult to determine accurately. The distributions shown are therefore normalized in each case to the data. The percentage contribution of the "Drell-type" diagrams was 54% at 1.825 GeV/c and 71% at 2.11 GeV/c, in good agreement with Ferrari's results of 72 and 66%.

Figure 6 shows the proton c.m. angular distribution for various selections of spectator momentum. At 1.825 GeV/c, where the small number of events precludes any selection, the OPEM calculation fits the data quite well. At 2.11 GeV/c, the agreement is good for events with spectator momentum < 150 MeV/c, which include very few double-scattering events. Even the distribution for spectators with momentum > 150 MeV/c still shows some forward-backward peaking, and only when the cut is pushed up to 250 MeV/c does it finally disappear. (With this cut almost all the events will involve double scattering.) A rough estimate of the degree of peripheralism is given by the percentage of events with $|\cos\theta| > 0.8$, and Table IV presents these data for the distributions of Fig. 6 and for the pp experiments. Since we expect less peripheralism at lower energies, the present experiment seems to be in agreement with the others. In Fig. 7 the distributions of the center-of-mass angles between particles, for events at 2.11 GeV/c with spectator momentum < 150 MeV/c, are compared with those of PRS. The agree-

²¹ The Fermi momentum of the proton in the deuteron causes a spread of full width 80–90 MeV about the central value.

²² E. Ferrari, Nuovo Cimento **30**, 240 (1963).

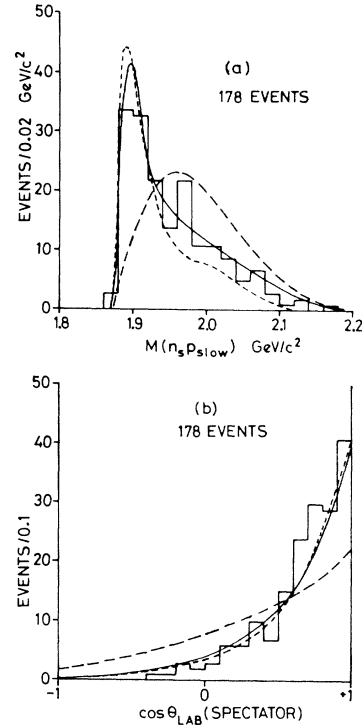


FIG. 5. Distributions for $n_s p p \pi^+ \pi^-$ events at 2.11 GeV/c with spectator momentum > 150 MeV/c: (a) invariant mass of spectator neutron and slower proton; (b) spectator-neutron angular distribution. The curves are the results of calculations using (i) statistical model (dashed), (ii) statistical model with final-state interaction (dotted, $C = 0.2$ GeV/c² for the 1S_0 state, 0.06 for 3S_1), and (iii) OPEM with final-state interaction (solid, $C = 0.12$ for 1S_0 , 0.04 for 3S_1).

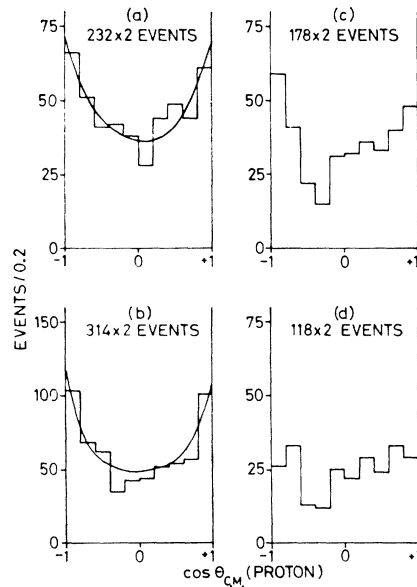


FIG. 6. Angular distribution of protons in the $p p \pi^+ \pi^-$ c.m. system, for $n_s p p \pi^+ \pi^-$ events: (a) at 1.825 GeV/c, all events; (b) at 2.11 GeV/c, spectator momentum < 150 MeV/c; (c) at 2.11 GeV/c, spectator momentum > 150 MeV/c; (d) at 2.11 GeV/c, spectator momentum > 250 MeV/c. The curves in (a) and (b) are from the OPEM calculations discussed in the text.

TABLE IV. Percentage of events with $|\cos\theta| > 0.8$ in the proton c.m. angular distribution for the reaction $pp \rightarrow pp\pi^+\pi^-$.

Experiment	pp c.m. energy (GeV/c)	Spectator-momentum cut (MeV/c)	Percentage of events with $ \cos\theta > 0.8$	OPEM prediction
Present experiment	2.369	None	27 ± 2	27.0
	2.469	<150	32 ± 2	28.7
		>150	30 ± 3	...
		>250	19 ± 3	...
Pickup <i>et al.</i> ^a	2.697	...	41 ± 2	...
Hart <i>et al.</i> ^b	2.978	...	56 ± 3	...

^a Reference 5(a).
^b Reference 5(b).

ment is very good, especially for the angle between protons.

The invariant-mass plots and the OPEM predictions at 2.11 GeV/c are shown in Fig. 8. The $\Delta^{++}(1236)$ is present in the $p\pi^+$ system, but the peak is shifted somewhat towards low-mass values. A least-squares fit, allowing for the variation of resonance width with energy,²³ puts the proportion of resonance at $(45 \pm 5)\%$, or rather less than that found in PRS. The $p\pi^+\pi^-$ system shows no evidence of $\Lambda^*(1470)$ or $\Lambda^*(1512)$ production. There is insufficient energy to produce the $\Lambda^*(1688)$.

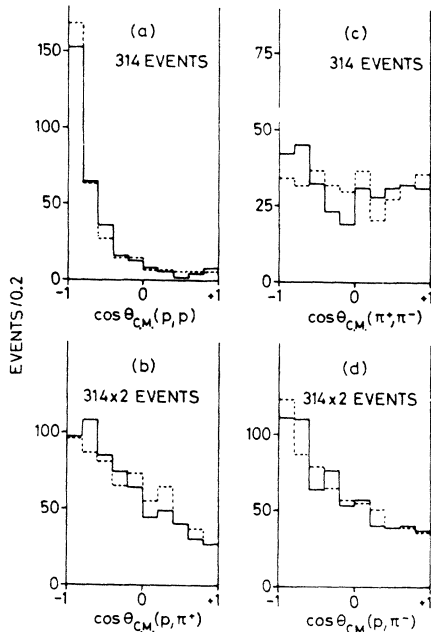


FIG. 7. Comparison of angles between particles in the $pp\pi^+\pi^-$ c.m. system for $n_s pp\pi^+\pi^-$ events at 2.11 GeV/c with spectator momentum < 150 MeV/c (solid histograms) and $pp \rightarrow pp\pi^+\pi^-$ events at 2.78 GeV/c [dotted histograms, taken from Ref. 5(a)]: (a) $p-p$; (b) $p-\pi^+$; (c) $p-\pi^-$; (d) $\pi^+-\pi^-$. The dotted histograms, based on 681 events, have been normalized to the same area as the solid ones.

²³ J. D. Jackson, Nuovo Cimento 34, 1644 (1964).

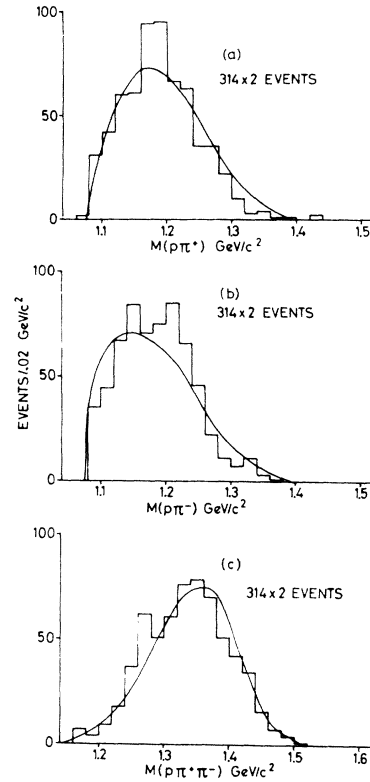


FIG. 8. Invariant-mass plots for $n_s pp\pi^+\pi^-$ events at 2.11 GeV/c with spectator momentum < 150 MeV/c: (a) $p\pi^+$; (b) $p\pi^-$; (c) $p\pi^+\pi^-$. The curves are OPEM predictions.

The presence of a spectator neutron seems therefore to have little effect on the $pp \rightarrow pp\pi^+\pi^-$ reaction, if events with very fast spectators, for which the impulse approximation is invalid, are excluded. The interaction is less peripheral than at the slightly higher energies of the pp experiments and there is less resonance production, but both effects may be naturally accounted for by the fact that the energies of this experiment are low, and comparatively near the threshold for double-pion production.

D. Summary

We have seen above that the spectator-nucleon momentum and angular distributions can be understood, qualitatively at least, in terms of the addition of a proportion of double-scattering events to the usual predictions of the impulse model. The proportion needed is larger for double-pion-production reactions than for single-pion production. Final-state interactions involving the spectator have more effect on the spectator's angular distribution than on its momentum. The comparison of the reactions $pd \rightarrow n_s pp\pi^+\pi^-$ and $pp \rightarrow pp\pi^+\pi^-$ suggests that the impulse approximation is valid if events with spectator momentum > 150 MeV/c are excluded.

This cut includes almost all the genuine impulse-

approximation events (88% using the Hulthén wave function, 86.3% with the repulsive core), but only very few of the double-scattering ones (4.1% for the $n_s p p \pi^+ \pi^-$ final state, 2.5% for $p_s p p \pi^-$, both at 2.11 GeV/c). It has been used in other bubble-chamber experiments²⁴ with deuteron targets. For these reasons, it was applied to the $p_s p p \pi^-$ events in this experiment.

For the other important final state involving a spectator, $p_s n p \pi^+ \pi^-$, the low-momentum spectators are missing. In order to retain a sufficient number of events at 2.11 GeV/c, the spectator-momentum cut had to be raised to 200 MeV/c, thereby increasing the contamination of double-scattering events. At 1.825 GeV/c, spectator-momentum selection had to be altogether abandoned.

IV. CROSS SECTIONS

From the total track length scanned in the experiment and the density of the deuterium, the number of events equivalent to a cross section of 1 mb was found to be 591 ± 12 at 1.825 GeV/c and 563 ± 12 at 2.11 GeV/c. Before using this conversion the numbers of events given in Table I must be corrected for the scanning efficiency, and in order to obtain free-nucleon cross sections there are also corrections due to the structure of the deuteron target.

The treatment of these corrections has been based on the work of Franco and Glauber.^{10(a)} By combining their expressions for the total and scattering cross sections, the absorptive part of the pd cross section may be written as

$$\sigma_{\text{abs}} = \sigma_{n \text{ abs}} + \sigma_{p \text{ abs}} - \frac{2}{k^2} \int S(\mathbf{q}) \{ \text{Re}[f_n(\mathbf{q}) f_p^*(\mathbf{q})] - \text{Re}[f_n(\mathbf{q}) f_p(-\mathbf{q})] \} d^{(2)}\mathbf{q} + \Phi.$$

The first two terms are the total absorption cross sections for free nucleons and include the partial cross sections which we wish to determine, the third is the contribution to double scattering from the shadowing effect, and the last includes the remaining contributions from double scattering and the effect of interference between single and double scattering. We have assumed that this last term is identical with the double-scattering background found in the least-squares fitting to the spectator momentum distributions. (For the double-pion-production final states with spectator protons, the spectator-momentum plot above 150 MeV/c was assumed to have the same proportion of double-scattering to impulse-approximation events as the $n_s p p \pi^+ \pi^-$ distribution in the same momentum range.)

By using the optical theorem, the shadowing-effect

²⁴ For example, P. Anninos, L. Gray, P. Hagerty, T. Kalogeropoulos, S. Zenone, R. Bizarri, G. Ciapetti, M. Gaspero, I. Laakso, S. Lichtman, and G. C. Moneti [Phys. Rev. Letters **20**, 402 (1968)] find that, in p - n annihilation at rest, the proton may be treated as a spectator up to 150 MeV/c, but not for higher momenta.

TABLE V. Free-nucleon cross sections.

Reaction	Cross section (mb)	
	1.825 GeV/c	2.110 GeV/c
$pn \rightarrow pp\pi^-$	2.57 ± 0.14	2.68 ± 0.19
$pn \rightarrow pp\pi^-\pi^0$	0.16 ± 0.03	0.35 ± 0.04
$pn \rightarrow pn\pi^+\pi^-$	0.77 ± 0.07	1.75 ± 0.20
$pp \rightarrow pp\pi^+\pi^-$	0.30 ± 0.03	0.66 ± 0.10
$pn \rightarrow d\pi^+\pi^-$	0.13 ± 0.03	0.17 ± 0.03
$pd \rightarrow pd\pi^+\pi^-$ ^a	0.18 ± 0.02	0.17 ± 0.02

^a Events not containing a spectator nucleon. For details see Ref. 6.

contribution for the whole of σ_{abs} , $\delta\sigma_{\text{abs}}$, in the limit of scattering by black spheres, may be written as $(\frac{1}{8}\pi)\sigma_n\sigma_p\langle r^{-2} \rangle_d$, where σ_n and σ_p are total cross sections on free nucleons and $\langle r^{-2} \rangle_d$ is the mean-inverse-square radius of the deuteron. In the absence of any information on the distribution of $\delta\sigma_{\text{abs}}$ between the various reaction channels, we have assumed that the neutron and proton shadowing is equal and that the shadowing effect for any absorptive reaction is proportional to its share of the total absorption cross section. We can then work out the correction factor by considering the known total absorption cross section for free protons and assuming the shadowing effect for this cross section to be one-half of $\delta\sigma_{\text{abs}}$. Using the experimental values of the cross sections,²⁵ and taking $\langle r^{-2} \rangle_d = 0.034 \text{ mb}^{-1}$,² we obtain correction factors of 1.19 at 1.825 GeV/c and 1.22 at 2.11 GeV/c for all our cross sections.

The cross sections for reactions on free nucleons which are obtained after the application of these corrections are given in Table V. Because of the Fermi momentum of the nucleons inside the deuteron, they represent an average over a c.m. energy distribution with full width 90 MeV, centered on the nominal value obtained from the beam momentum. The cross sections are plotted as a function of energy in Fig. 9, along with the results of experiments at nearby energies. Table V

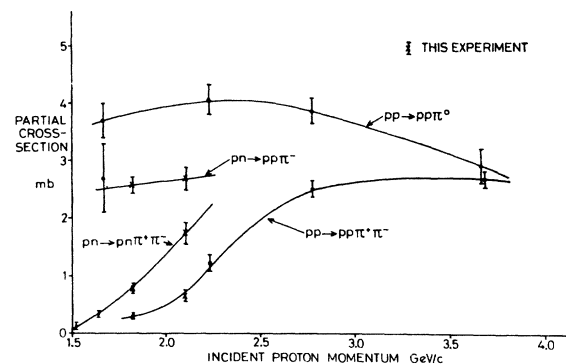


FIG. 9. Single- and double-pion-production cross sections as a function of incident proton momentum. The pp cross sections are taken from Ref. 5 and the present work, the pn cross sections from Ref. 1 and the present work. The curves merely join up the experimental points.

²⁵ V. S. Barashenkov and V. M. Maltsev, Fortschr. Physik **9**, 549 (1961).

also includes previously published⁶ cross sections for events with final-state deuterons.

The $T=0$ contribution to the reaction $pn \rightarrow pp\pi^-$ is given by $\sigma(pn \rightarrow pp\pi^-) - \frac{1}{2}\sigma(pp \rightarrow pp\pi^0)$. Taking the average of our two values for $\sigma(pn \rightarrow pp\pi^-)$, and comparing it with the average of the published values of $\frac{1}{2}\sigma(pp \rightarrow pp\pi^0)$ at kinetic energies of 970,^{5(c)} 1480,^{5(d)} and 2000 MeV,^{5(a)} a proportion of $(26 \pm 7)\%$ $T=0$ is obtained, in agreement with the 35–40% found previously at 970 MeV.¹ Similarly, the $T=0$ part of the reaction $pn \rightarrow pn\pi^+\pi^-$ is given by $\sigma(pn \rightarrow pn\pi^+\pi^-) - \frac{3}{8}\sigma(pp \rightarrow pp\pi^+\pi^-)$, and is, from Table V, 0.53 ± 0.10 mb at 1.825 GeV/c and 1.45 ± 0.20 mb at 2.11 GeV/c. The increase of 0.92 ± 0.22 mb between the two momenta therefore accounts for some, at least, of the 3-mb rise observed in the $T=0$ total cross section² over the same range of momentum. The proportion of $T=0$ state in the reaction $pn \rightarrow pn\pi^+\pi^-$ is large, $(69 \pm 13)\%$ at 1.825 GeV/c and $(83 \pm 15)\%$ at 2.11 GeV/c, which also agrees with previous work at slightly lower energies. Dominance of double-pion production by the $\Delta(1236)$ produced from a state of $T=0$ leads¹ to an expected ratio $\sigma(pn \rightarrow pn\pi^+\pi^-)/\sigma(pn \rightarrow pp\pi^-\pi^0)$ of 5/1. Our results for this ratio are 4.4 ± 1.0 and 5.0 ± 0.8 , in excellent agreement.

V. $pn \rightarrow pp\pi^-$

The events concerned are of the type $pd \rightarrow p_s pp\pi^-$ with a spectator-momentum cut at 150 MeV/c to purify the sample. The experimental distributions are compared with predictions of the statistical model and of a Ferrari Selleri-type²⁶ OPEM, allowance being made in each case for the variation in $pp\pi^-$ c.m. energy produced by the Fermi momentum of the neutron. The possible one-pion-exchange diagrams are shown in Fig. 10. No one diagram is dominant from isospin considerations, so contributions from all four have been added. Interference terms have been neglected, since they are expected^{26(b)} to be zero in some cases and small in the remainder. The form-factor

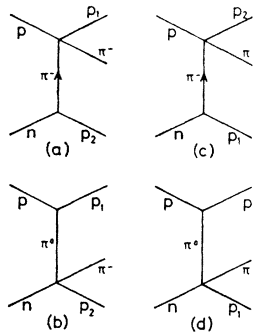


FIG. 10. Possible one-pion-exchange diagrams for the reaction $pn \rightarrow pp\pi^-$.

²⁶ (a) E. Ferrari and F. Selleri, *Nuovo Cimento Suppl.* **24**, 453 (1962); (b) **27**, 1450 (1963).

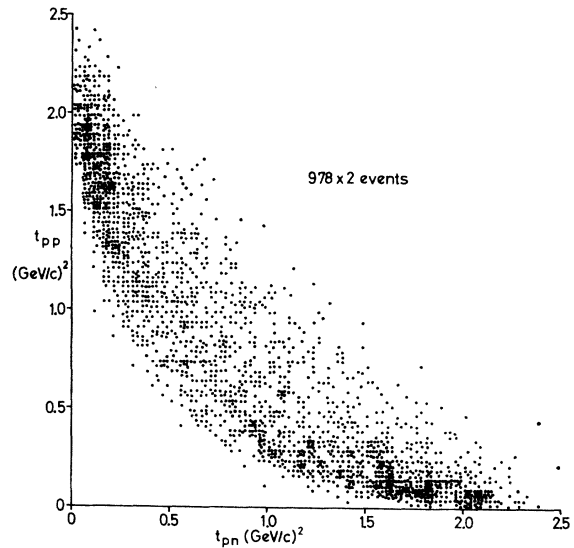


FIG. 11. Scatter plot of momentum transfers between initial and final-state nucleons. For each final-state proton, the momentum transfer to the incident proton is plotted against the momentum transfer to the neutron.

expressions obtained by Ferrari and Selleri from pp scattering between 1 and 3 GeV have been used. The calculated total cross sections for $pn \rightarrow pp\pi^-$ are 2.62 mb at 1.825 GeV/c and 2.76 mb at 2.11 GeV/c in good agreement with the experimental values in Table V. The other distributions have been normalized to the data.

At 7 GeV/c,⁴ it was found easy to assign the two final-state protons to the top or bottom vertex of Fig. 10 on momentum-transfer considerations. In our ex-

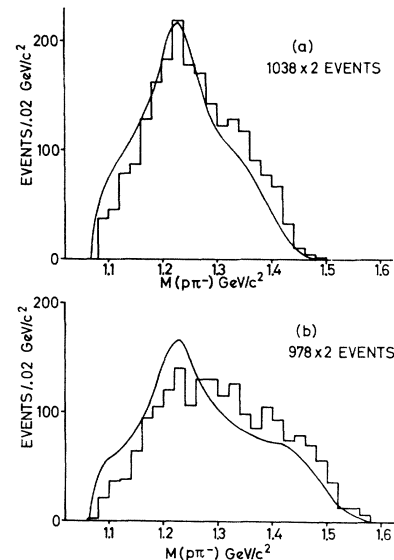


FIG. 12. $p\pi^-$ invariant-mass plots for $p_s pp\pi^-$ events with spectator momentum < 150 MeV/c at (a) 1.825 and (b) 2.11 GeV/c. The curves are OPEM predictions.

periment, the separation is not so clean, as Fig. 11 demonstrates. If the separation is attempted, the invariant-mass plots for $p_p\pi^-$ and $p_n\pi^-$ (in the notation of Ref. 4, where each final-state proton is labeled according to its association with one of the initial nucleons) are not very different; both show the presence of some $\Delta^0(1236)$ and have no clear evidence for $N^*(1470)$, which would, however, only appear at the upper limit of phase space.

Figure 12 shows the $p\pi^-$ invariant-mass plots. There is obviously a considerable proportion of $\Delta^0(1236)$ present, and the proportions obtained in a least-square fit are $(50\pm 5)\%$ at 1.825 GeV/c and $(40\pm 10)\%$ at 2.11 GeV/c. The OPEM predictions are in good agreement with experiment, and this holds also for the laboratory-kinetic-energy plots shown in Fig. 13. Figure 14 contains the angular distributions of particles in the c.m. system and shows forward-backward peaking in the proton distribution, due to the peripheral nature of the reaction. The proportion of events with $|\cos\theta| > 0.8$ is $(40.9\pm 1.4)\%$ at 1.825 GeV/c and $(45.7\pm 1.5)\%$ at 2.11 GeV/c, compared with OPEM predictions of 42.2 and 48.7%.

The general agreement with the OPEM predictions is remarkably good. The calculations have used experimental π^-p and π^0p cross sections which of course include contributions from $\Delta(1236)$ production. However, the $T=0$ part of the $p-n$ interaction cannot take part in a reaction $pn \rightarrow \Delta^0p$, by isospin conservation, and to this extent the OPEM calculation must be incorrect. The $pn \rightarrow pp\pi^-$ and $pp \rightarrow pp\pi^0$ cross sections suggest that the proportion of $T=0$ is 26%, as we saw above, so it is surprising to see such good agreement with experiment.

There are two other ways of assessing the $T=0$ part of the cross section. If the reaction $pn \rightarrow pp\pi^-$ goes completely from the $T=1$ state, not only the cross sections but also the detailed angular and energy distributions of $pn \rightarrow pp\pi^-$ and $pp \rightarrow pp\pi^0$ should be identical (apart from a factor of $\sqrt{2}$ in the amplitude). There is no pp experiment at our exact energies, the nearest with published data on $pp\pi^0$ events being at 970 MeV.^{5(c)} Figure 15 shows that good agreement is found for the angular distributions.

The existence of nonzero and nonorthogonal $T=0$ and $T=1$ amplitudes in $pn \rightarrow pp\pi^-$ leads¹ to the prediction of forward-backward asymmetry between the final-state protons. Counting protons in the forward and backward hemispheres gives asymmetries of 0.010 ± 0.038 at 1.825 GeV/c and 0.057 ± 0.039 at 2.11 GeV/c, which are both compatible with zero. Going further, we can separate the protons into p_F and p_B , according to which is the more forward or backward in the c.m. system, and then compare their distributions. Figure 16 shows that the $p_F\pi^-$ and $p_B\pi^-$ angular correlations are virtually identical and agree well with the OPEM predictions. Other distributions also fail to distinguish

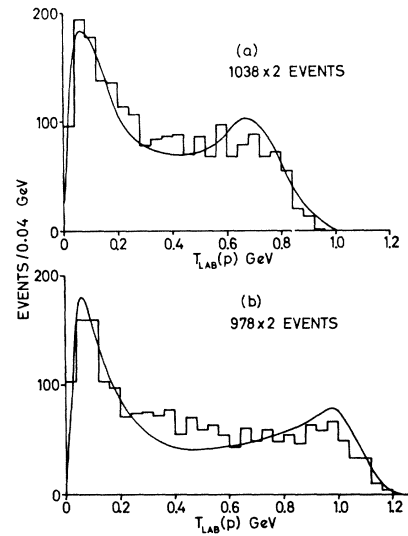


FIG. 13. Proton laboratory-kinetic-energy plots for $pp\pi^-$ events with spectator momentum < 150 MeV/c at (a) 1.825 and (b) 2.11 GeV/c, together with OPEM predictions.

any difference between p_F and p_B , so that there is no clear indication of a significant $T=0$ amplitude.

Thus, the evidence for a considerable proportion of $T=0$ part to the reaction comes solely from the cross-

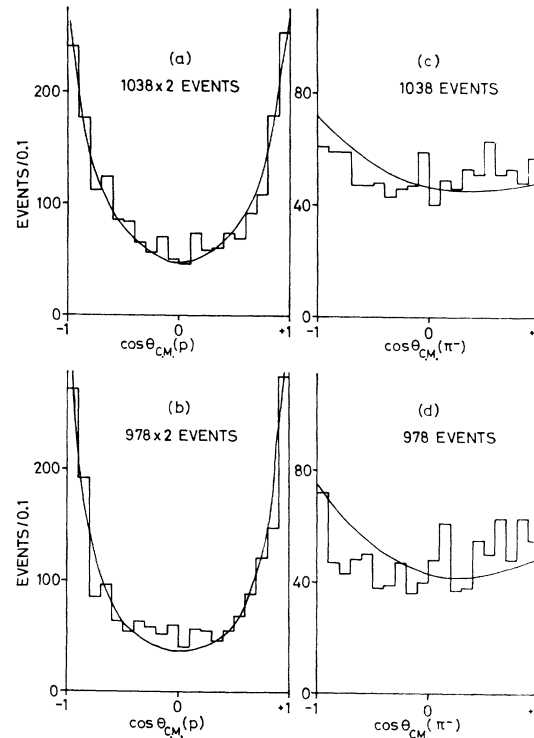


FIG. 14. Angular distributions in the $pp\pi^-$ c.m. system for $pp\pi^-$ events with spectator momentum < 150 MeV/c, together with OPEM predictions: (a) protons at 1.825 GeV/c; (b) protons at 2.11 GeV/c; (c) π^- at 1.825 GeV/c; (d) π^- at 2.11 GeV/c.

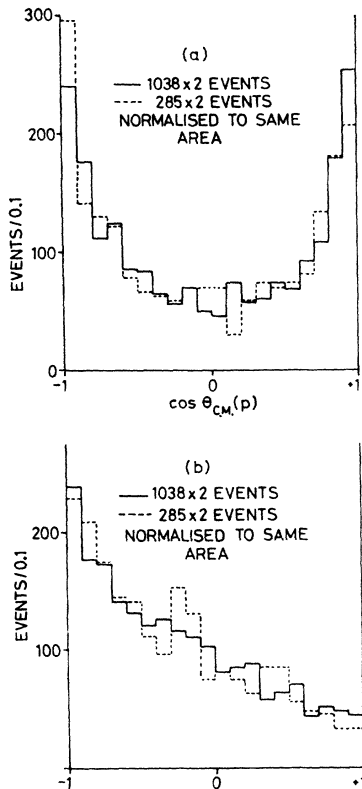


FIG. 15. Comparison of angular distributions in the $pp\pi^-$ c.m. system for $p_s pp\pi^-$ events at 1.825 GeV/c with spectator momentum <150 MeV/c (solid histogram) and $pp \rightarrow pp\pi^0$ events at 1.67 GeV/c [dotted histograms, taken from Ref. 5(c)]: (a) proton c.m. angle; (b) angle between p, π^- or p, π^0 .

section values and seems to be in disagreement with the rest of the evidence. A similar situation was found at 970 Mev,¹ in an experiment with incident neutrons in a hydrogen bubble chamber.

VI. $pn \rightarrow np\pi^+\pi^-$

The events here come from the final state $p_s n p \pi^+ \pi^-$. As explained above, the absence of events with low-momentum spectators leads to a fairly large contamination with double-scattering events. At 2.11 GeV/c, where a spectator-momentum cut of 200 MeV/c has been applied, the contamination is still estimated at 12%.

There are two types of one-pion-exchange diagrams for this reaction: "double-isobar" graphs in which the two pions are at different vertices and "Drell-type" ones in which both pions are at the same vertex. The three double-isobar diagrams are shown in Fig. 17. At our energies the $T = \frac{3}{2}$ state of the pion-nucleon system is dominant, because of the large cross sections for $\Delta(1236)$ formation, and its contributions to diagrams (a)–(c) are found, from the Clebsch-Gordan coefficients, to be in the ratio 81:1:4. Diagram (a) is therefore expected to have by far the largest contribution to the

calculation, dwarfing those from the other double-isobar and Drell diagrams. Considering this, and the small number of events in our sample (as well as the high contamination), we have assumed it a valid approximation to calculate only diagram (a). The methods and the form factors of Ferrari and Selleri²⁶ were used and the effect of the spectator proton on the $np\pi^+\pi^-$ c.m. energy allowed for. Statistical-model calculations were also carried out allowing for this effect.

Figure 18 shows the combined c.m. angular distributions for proton and neutron. (This distribution corresponds to that for the proton c.m. angle in $pp \rightarrow pp\pi^+\pi^-$.) At 1.825 GeV/c the forward-backward peaking is slight, owing to the combination of low energy and high contamination, but at 2.11 GeV/c there is evidence of peripheralism. Our usual index, the percentage of events with $|\cos\theta| > 0.8$, gives experimental values of $(23 \pm 2)\%$ at 1.825 GeV/c and $(30 \pm 3)\%$ at 2.11 GeV/c, in fairly good agreement with theoretical predictions of 25.9 and 31.5%. The degree of peripheralism seems to be slightly less than that found above in $pp \rightarrow pp\pi^+\pi^-$ at the same energies.

The 2.11-GeV/c invariant-mass plots are shown in Fig. 19, and while differing appreciably from phase space, are on the whole in good agreement with the OPEM calculations. Similar behavior is found at 1.825

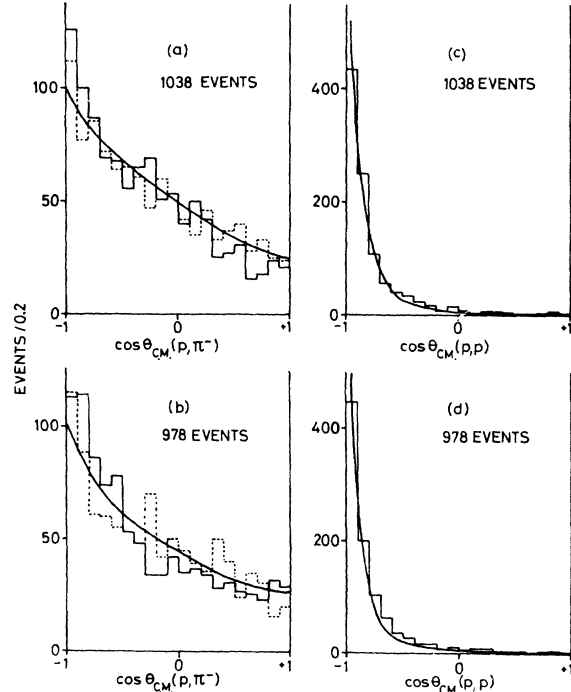


FIG. 16. Angles between particles in the $pp\pi^-$ c.m. system for $p_s pp\pi^-$ events with spectator momentum <150 MeV/c: (a) $p_F \pi^-$ (solid) and $p_B \pi^-$ (dotted) at 1.825 GeV/c; (b) $p_F \pi^-$ (solid) and $p_B \pi^-$ (dotted) at 2.11 GeV/c; (c) $p-p$ at 1.825 GeV/c; (d) $p-p$ at 2.11 GeV/c. p_F is defined as the more forward proton in the c.m. system and p_B as the more backward. The curves are OPEM predictions.

GeV/c. The $\Delta(1236)$ is prominent in the $p\pi^+$ and $n\pi^-$ plots, as expected. The $p\pi^+\pi^-$ and $n\pi^+\pi^-$ invariant-mass plots show an excess of events above phase space around 1400–1500 MeV/c², but the OPEM calculation, which uses only the experimental π^+p elastic scattering cross section (i.e., pure $T=\frac{3}{2}$), fits the data well. We conclude, therefore, that the excess over phase space is a kinematic reflection of $\Delta(1236)$ production, and there is no evidence for the presence of $N^*(1470)$. This is perhaps not very surprising, since $N^*(1470)$ production falls off rapidly with increasing momentum transfer²⁷ and typical momentum transfers in this experiment are 0.4–0.6 (GeV/c)².

If the threshold for $N^*(1470)$ production were responsible for the rise in the total $T=0$ nucleon-nucleon cross section, we would expect to see its $N\pi\pi$ decay modes strongly in this final state. It seems, therefore, that although the reaction $np \rightarrow np\pi^+\pi^-$ accounts for a significant portion of the cross-section rise, it is not in the form of a reaction $pn \rightarrow NN^*(1470)$.

At 3.7 GeV/c, Cohn *et al.*^{3(b)} have observed that a significant part of the reaction $pn \rightarrow np\pi^+\pi^-$ proceeds through $pn \rightarrow \Delta^{++}\Delta^-$, with a substantial amount of $Q=2$ exchange. Unfortunately, the present experiment is only just above threshold for production of two isobars and we have not found it possible to say anything meaningful about the possibility of $Q=2$ exchange.

VII. CONCLUSIONS

The impulse approximation is valid up to a spectator momentum of 150 MeV/c. For higher momenta there

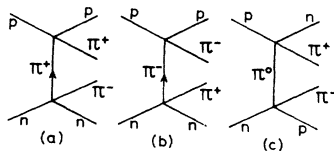


FIG. 17. Double-isobar one-pion-exchange diagrams for the reaction $pn \rightarrow pn\pi^+\pi^-$.

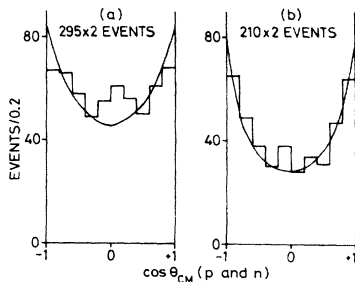


FIG. 18. Combined plot of proton and neutron angles in the $pn\pi^+\pi^-$ c.m. system for $p_n pn\pi^+\pi^-$ events: (a) at 1.825 GeV/c, for all events; (b) at 2.11 GeV/c, for events with spectator momentum <200 MeV/c. The curves are OPEM predictions.

²⁷ See, e.g., L. di Lella, in *Proceedings of the Heidelberg International Conference on Elementary Particles*, edited by H. Filthuth (North-Holland Publishing Co., Amsterdam, 1968).

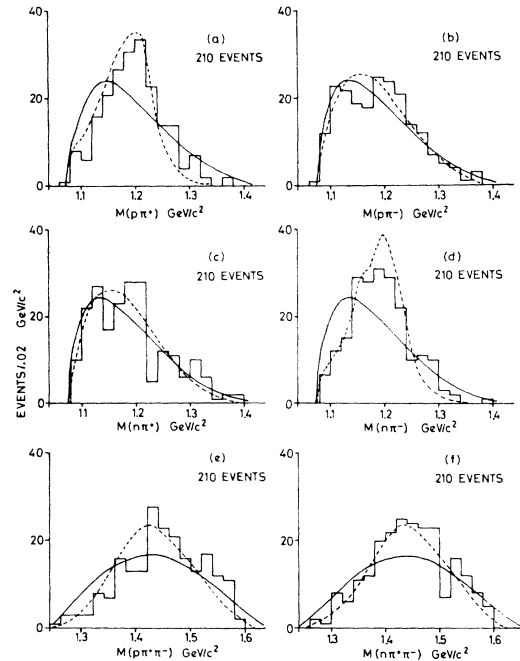


FIG. 19. Invariant-mass plots for $p_n pn\pi^+\pi^-$ events at 2.11 GeV/c with spectator momentum <200 MeV/c: (a) $p\pi^+$; (b) $p\pi^-$; (c) $n\pi^+$; (d) $n\pi^-$; (e) $p\pi^+\pi^-$; (f) $n\pi^+\pi^-$. The solid curves are statistical-model predictions and the dashed curves OPEM predictions.

is considerable double scattering, this being larger for double-pion production.

Results for the reaction $pn \rightarrow pp\pi^-$ are generally in good agreement with one-pion exchange. The usual estimate of the proportion of $T=0$ in the reaction from the $pn \rightarrow pp\pi^-$ and $pp \rightarrow pp\pi^0$ cross sections seems to be larger than other evidence would suggest.

The cross section for the reaction $pn \rightarrow np\pi^+\pi^-$ increases sufficiently between 1.825 and 2.11 GeV/c to account for one-third of the total increase in the $T=0$ nucleon-nucleon cross section over the same momentum range. There is no evidence that this reaction proceeds via $pn \rightarrow NN^*(1470)$.

ACKNOWLEDGMENTS

We would like to thank the operating crews of the NIMROD proton synchrotron and the Saclay deuterium bubble chamber for their assistance in carrying out the experiment, and our measuring staff at Cambridge for their efforts in the film analysis. We have had useful discussions with Dr. K. F. Riley and Dr. J. G. Rushbrooke throughout the course of the experiment. One author (D. C. B.) wishes to acknowledge financial support from the National Institute for Research in Nuclear Science and Clare College, Cambridge, and another (M. J. C.) financial support from the Science Research Council.